Spectroscopic and Theoretical Investigation of (*R*)-3-Methylcyclopentanone. The Effect of Solvent and Temperature on the Distribution of Conformers

Watheq Al-Basheer,[†,‡] Richard M. Pagni,[§] and Robert N. Compton*[,†,§]

Departments of Physics and Chemistry, University of Tennessee, Knoxville, Tennessee 37996

Received: December 4, 2006; In Final Form: January 18, 2007

Temperature-dependent electronic circular dichroism (CD) spectra are reported for (*R*)-(+)-3-methylcyclopentanone (*R*3MCP) in 34 solvents. Analysis of these data yielded the enthalpy and entropy differences between axial methyl and equatorial methyl conformers, the dominant conformers for *R*3MCP. The weakly absorbing $n \rightarrow \pi^*$ transition exhibited a decrease in λ_{max} as the solvent polarity increased. Vibrational CD fine structure of the $n \rightarrow \pi^*$ transition was observed in the gas phase in addition to several of the solvents. Vapor-phase CD spectra were compared to both the solution-phase spectra and theoretical calculations of the axial and equatorial methyl conformers. Optical rotation (OR) measurements for *R*3MCP in cyclohexane solution in the visible region showed excellent agreement with OR DFT calculations of the equatorial and axial methyl conformers. Density functional calculations with B3LYP and the 6-13G* and aug-cc-pVDZ basis sets, which incorporate the solvent dielectric constant, yielded trends in thermodynamic quantities as a function of polarity and solvent dipole moments that are only weakly or not observed in experiments.

Introduction

Conformational analysis of ketones containing five-membered rings has been performed using various spectroscopic techniques including NMR spectroscopy,[1] IR spectroscopy,[2,3] electron diffraction,[4] and vibrational circular dichroism (VCD).[3] Electronic CD, which is the differential absorption of left and right circularly polarized light (LCPL and RCPL) by a molecule, has been used in the conformational analysis of five-membered rings as well. Over 40 years ago, Djerassi and co-workers reported the first temperature-dependent CD measurements on a variety of dissymmetric molecules including ketones.[5−12] Many other studies of solvent effects on the chirooptical properties of ketones have been reported in the literature.[13,14]

3-Methylcyclopentanone is a chiral ketone that can exist in as many as five conformers.[3,15−18] However, at room temperature, the structural populations are dominated by two conformers having a twisted five-membered ring with equatorial and axial methyl groups.[15] Kim and Baer determined the enthalpy difference between the two conformers in the gas phase using a multiphoton ionization technique[19] ($\Delta H° = 4.97 \pm 0.59$ kJ/mol). Later, Polavarapu and co-workers determined the enthalpy difference between the two conformers of neat (*R*)-(+)-3-methylcyclopentanone (*R*3MCP) using temperature-dependent infrared spectroscopy[3] and found $\Delta H° = 4.84 \pm 0.08$ kJ/mol. In both cases, the conformer with the equatorial methyl group was dominant. Because of our interest in the spectroscopy of *R*3MCP in the gas phase[20] and the influence of solvent on the optical rotation of chiral molecules,[21] we thought it would be a fruitful endeavor to measure the effect of solvent on the distribution of the two major conformers by temperature-dependent electronic CD. This is feasible because *R*3MCP is commercially available and is miscible in a wide range of solvents. Density functional calculations of the CD spectra for the equatorial and axial forms as a function of the dielectric constant of the solvent were also carried out using the Gaussian 03 software package.

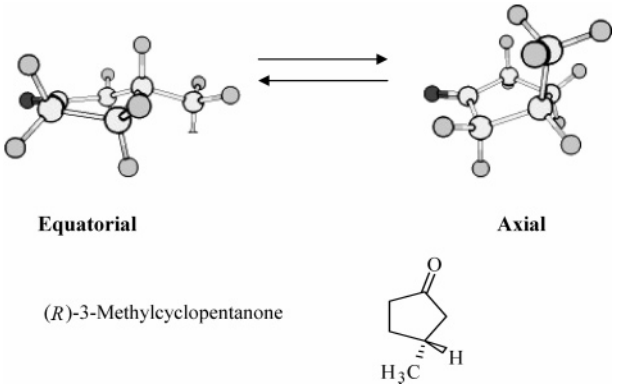

Experimental

(*R*)-3-methylcyclopentanone was purchased from the Sigma-Aldrich Chemical Co. and used without further purification. All solvents used in this study were commercially available and were used as received. A typical concentration used in the CD solution studies was 2.6×10^{-2} M. CD spectra were obtained using a temperature-controlled Aviv model 202 series CD spectrometer employing quartz cuvettes. The vapor-phase CD spectra of the two dominant conformers of *R*3MCP are shown in Figure 1 and consist of a net positive $n \rightarrow \pi^*$ CD transition at ~300 nm and a negative $n \rightarrow 3s$ transition below 200 nm. The optical rotatory dispersion (ORD) of *R*3MCP in cyclohexane was recorded on a Perkin-Elmer 241 polarimeter. The polarimeter is restricted to five wavelengths, two of which are generated from a sodium lamp ($\lambda = 589$ and 578 nm) and the

* To whom correspondence should be addressed. E-mail: rcompton@utk.edu.
† Department of Physics.
‡ Present address: Department of Physics, The Hashemite University, Jordan.
§ Department of Chemistry.

10.1021/jp068320d CCC: $37.00
Published on Web 03/03/2007

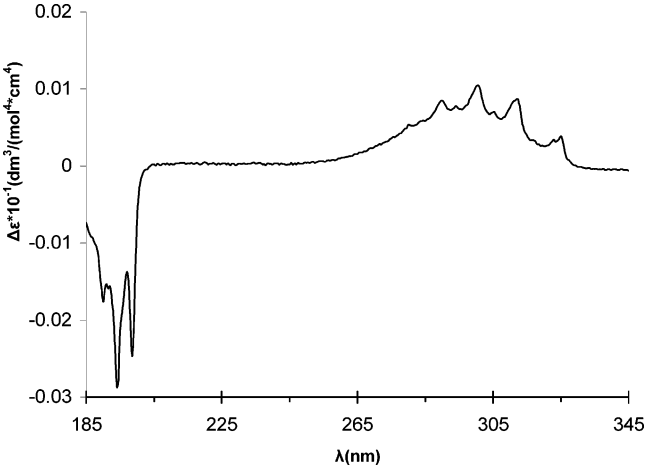

Figure 1. CD spectrum in for *R*3MCP in the vapor phase at room temperature.

other three of which are from a mercury lamp (λ = 546, 436, and 365 nm). Calculations of the CD spectra and ORD values for the axial and equatorial conformers, as well as their solvent effects, were carried out using the Gaussian 03 package of programs.[22]

The analysis of the CD data was carried out in the following manner: The CD signal is a measure of the difference in extinction coefficients, $\Delta\epsilon$, of an optically active molecule exposed to left and right circularly polarized light (LCPL and RCPL). In cases where only two conformers, axial (a) and equatorial (e), are involved, or in cases where there are more than two conformers in equilibrium but where the system is dominated by two of them, the observed CD signal (area under the $n \rightarrow \pi^*$ peak) at a given temperature is related to the CD signals of the equatorial and axial forms and their corresponding mole fractions as follows

$$\Delta\epsilon_{obs}(T) = f_e\Delta\epsilon_e + f_a\Delta\epsilon_a \quad (1)$$

The free energy difference between the two conformers is related to their mole fractions by

$$\Delta G = -RT \ln K = -RT \ln\left(\frac{f_a}{f_e}\right) \quad (2)$$

It follows from eq 2 that the following is true

$$f_e = 1 - f_a = 1 - f_e e^{-\Delta G/RT} \quad (3)$$

Substituting eq 1 into eq 3 yields

$$\Delta\epsilon_{obs}(T) = \frac{\Delta\epsilon_e}{1 + e^{-\Delta G/RT}} + \frac{\Delta\epsilon_a e^{-\Delta G/RT}}{1 + e^{-\Delta G/RT}} \quad (4)$$

Extrapolation of eq 4 to T = 0 K affords

$$\Delta\epsilon_{obs}(T{=}0\ \text{K}) = \Delta\epsilon_e \quad (5)$$

and extrapolation to infinite temperature affords

$$\Delta\epsilon_{obs}(T{=}\infty) = \frac{\Delta\epsilon_e}{2} + \frac{\Delta\epsilon_a}{2} \quad (6)$$

From eqs 5 and 6, one can obtain the CD signals for the equatorial and axial forms in a given solvent. There is an inherent assumption that the CD for each conformer is not dependent on temperature. These extrapolations are close to

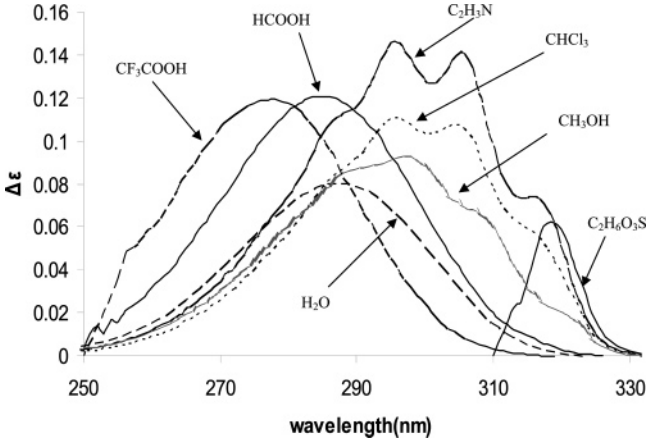

Figure 2. Room-temperature CD spectra, in dm^3/(mol^4 cm^4), of the $n \rightarrow \pi^*$ transition band for *R*3MCP. Wavelength maximum in solution: trifluoroacetic acid (CF_3COOH), 277 nm; formic acid (CHCOOH), 285 nm; water (H_2O), 287 nm; chloroform ($CHCl_3$), 295 nm; acetonitrile (C_4H_3N), 296 nm; methanol (CH_3OH), 297 nm; and dimethyl sulfite ($C_2H_6O_3S$), 319 nm.

linear and appear to be valid because the obtained values are approximately equal, but of opposite sign, to those predicted by theoretical B3LYP density functional calculations[20] using the 6-31G* basis set of the equatorial and axial conformers CD spectra. Once the CD signals of the two conformers have been obtained, one can calculate the mole fractions of each conformer at a given temperature. A van't Hoff plot of these data subsequently affords the differences in enthalpy, ΔH°, and entropy, ΔS°, between the two conformers in a given solvent.

It is easy to show that eq 4 can be written as

$$\Delta\epsilon_{obs}(T) = \Delta\epsilon(T{=}\infty) + [\Delta\epsilon(T{=}0) - \Delta\epsilon(T{=}\infty)] \tanh\left(\frac{\Delta G}{RT}\right) \quad (7)$$

This relationship is equivalent to that of Ballard, Mason, and Vane,[23] which was also used in conformational analysis, with the exception that our hyperbolic term contains ΔG° and theirs ΔH°. The reason for this discrepancy is unclear but might be simply due to the neglect of the $T\Delta S$° term in ref 23.

Density functional calculations of B3LYP type using the aug-cc-pVDZ basis set were carried out using the Gaussian 03 package of programs.[22]

Results and Discussion

The vapor-phase CD spectrum of *R*3MCP in the $n \rightarrow \pi^*$ region, with λ_{max} = 299 nm, exhibits considerable vibrational structure and substructure (see Figure 1). Because we were unable to ensure that all of the compound remained in the vapor state, it was not possible to determine the temperature-dependent CD of the vapor. This was not a problem when the CD spectra were determined in 34 different solvents of different dielectric constants, polarities, polarizabilities, and other properties.[24] The CD spectra of *R*3MCP at ambient temperature in several solvents are shown in Figure 2. There is an approximately linear correlation between λ_{max} and the polarity of the solvent, as expected for an $n \rightarrow \pi^*$ transition.[25] The correlation is less than perfect because the CD spectrum is a superposition of the CD spectra of the individual conformers, which are expected to show different influences of the solvents. The temperature-dependent CD spectra of *R*3MCP in cyclohexane, acetonitrile, acetic acid, and water are shown in Figure 3. In each case, the CD intensity decreases as the temperature of the sample is raised. This is a

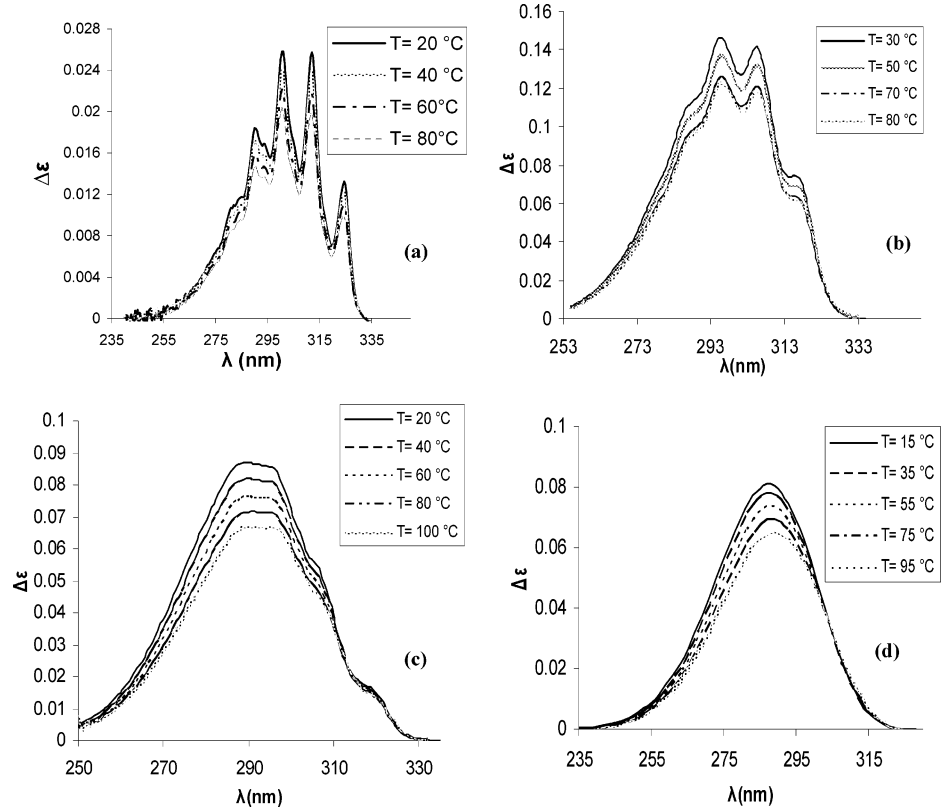

Figure 3. Temperature-dependent CD transition spectra ($n \rightarrow \pi^*$) in dm^3/(mol^4 cm^4) of *R*3MCP in (a) cyclohexane, (b) acetonitrile, (c) acetic acid, and (d) water.

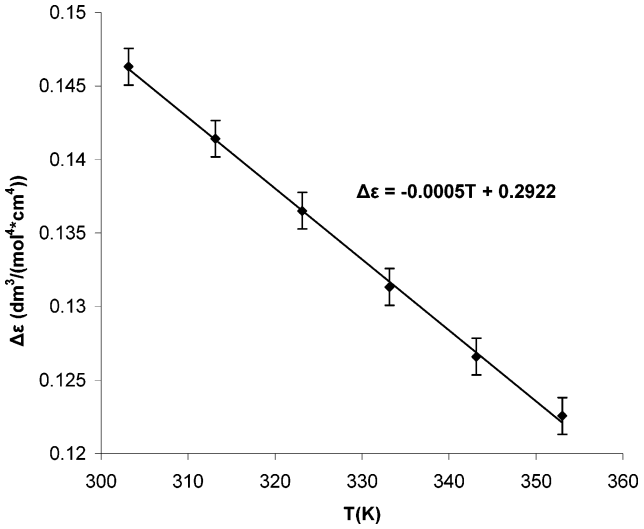

Figure 4. CD peak values for *R*3MCP in acetonitrile solution versus sample temperature, *T*. The *y* intercept is the CD signal due to the equatorial conformer.

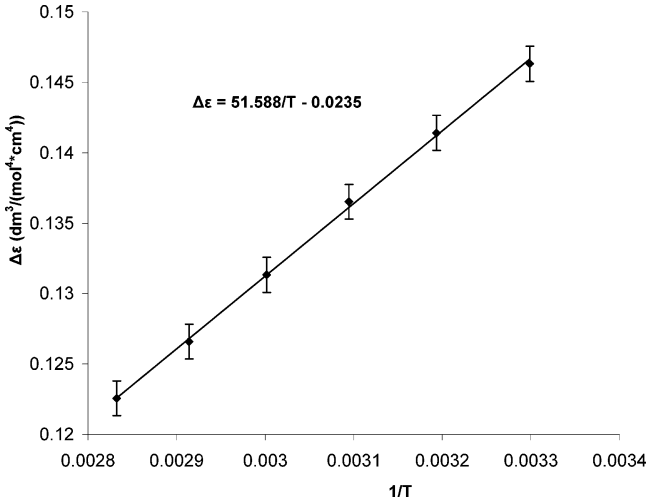

Figure 5. CD peak values for *R*3MCP in aceonitrile solution versus reciprocal of sample temperature, 1/*T*. The *y* intercept is due to the equal contributions of the equatorial and axial conformers.

previously known consequence of the fact that the equatorial conformer has a positive CD signal whereas the axial CD signal is negative. As the temperature is raised, the amount of the axial conformer increases at the expense of the equatorial conformer.

Typical extrapolated plots of the acetonitrile data to zero and infinite temperature are shown in Figures 4 and 5. In these cases, the correlations are linear but, as is evident from eq 4, need not have been so. As mentioned before, the near linearity in the $\Delta\epsilon$ versus T and $1/T$ plots is a consequence of the fact that the equatorial and axial conformers have CD signals that are approximately equal in magnitude but opposite in sign. From the *y* intercepts of the two plots and the use of eqs 5 and 6, we calculated that the CD signals for the equatorial and axial

TABLE 1: Mole Fraction Populations of Axial and Equatorial Conformers of *R*3MCP Solution in Acetonitrile as a Function of Sample Temperature

T (K)	$1/T$	$\Delta\epsilon$	f_a	f_e	$K = f_a/f_e$	ln K
303.15	0.0033	0.1463	0.231	0.769	0.3004	−1.2024
313.15	0.00319	0.1414	0.238	0.762	0.3137	−1.1591
323.15	0.00309	0.1365	0.246	0.754	0.3272	−1.1170
333.15	0.003	0.13133	0.254	0.746	0.3418	−1.0733
343.15	0.00291	0.1265	0.262	0.738	0.3555	−1.0341
353.05	0.00283	0.1225	0.268	0.732	0.3673	−1.0014

conformers in the $n \rightarrow \pi^*$ region are 0.2922 and −0.3392 dm^3/(mol^4 cm^4), respectively, values that are almost equal in absolute value but opposite in sign. From these values, the mole fractions of the two conformers at a measured temperature could be

TABLE 2: *R*3MCP Thermodynamic Constants in 34 Common Solutions Determined from Temperature-Dependent CD Measurements for the $n \rightarrow \pi^*$ Transition Band

solvent	$\Delta H°$ (kJ/mol)	$\Delta S°$ [J/(mol K)]	$\Delta G°$(298 K) (kJ/mol)	dielectric constant, ϵ_r[32,33]	$E_T(30)$[32,33] (kcal/mol)	Taft parameters[32,33] α	β	π^*	λ_{max} (nm)
cyclohexane	3.50	1.94	2.92	2.02[a]	30.9				300
benzene	3.45	1.94	2.87	2.27	34.3	0.00	0.10	0.55	299
toluene	3.62	1.95	3.04	2.38	33.9	0.00	0.11	0.49	310
chlorobenzene	3.67	1.95	3.09	5.62	36.8	0.00	0.07	0.68	298
hexafluorobenzene	3.35	1.90	2.78	2.05	34.2	0.00	0.02	0.27	297
chloroform	3.26	1.97	2.67	4.81[a]	39.1	0.20	0.10	0.58	295
carbon tetrachloride	3.30	1.94	2.72	2.24	32.4	0.00	0.10	0.21	300
tetrahydropyran	3.70	1.96	3.16	5.61	37.4	0.00	0.55	0.55	299
anisole	3.44	1.96	2.86	4.33	36.2	0.00	0.54	0.48	309
benzyl ether	3.69	2.01	3.09	3.86	36.3	0.00	0.41	0.80	309
acetonitrile	3.63	1.96	3.04	35.94	45.6	0.19	0.40	0.66	296
propionitrile	3.34	1.94	2.76	28.26	43.6	0.00	0.37	0.64	297
butyronitrile	3.39	1.93	2.81	24.83	42.5	0.00	0.45	0.63	297
valeronitrile	3.59	1.99	2.99	19.71	42.4	0.00		0.63	297
adiponitrile	3.56	1.94	2.98						296
crotononitrile	3.56	1.96	2.98						297
glutaronitrile	3.67	1.93	3.09						296
trimethylacetonitrile	3.61	1.95	3.03						298
dimethyl sulfoxide	3.71	1.95	3.13	46.45	45.1	0.00	0.76	1.00	297
dimethyl sulfite	3.43	1.94	2.85		41.5	0.00	0.45	0.7	319
formic acid	3.52	1.94	2.94	58.50	57.7	1.23	0.38	0.65	285
acetic acid	3.66	1.94	3.08	6.17[a]	55.2	1.12	0.45	0.64	290
trifluoroacetic acid	3.33	1.96	2.75	8.55		2.38		0.50	277
methanol	3.37	2.11	2.74	32.66	55.4	0.98	0.66	0.60	297
ethanol	3.21	1.81	2.67	24.55	51.9	0.86	0.75	0.54	298
2-propanol	3.48	2.17	2.83	19.92	48.4	0.76	0.84	0.40	300
isobutyl alcohol	3.43	1.94	2.85	17.93	48.6	0.79	0.84	0.40	299
2-butanol	3.32	1.89	2.76	16.56	47.1	0.69	0.80	0.40	300
t-butanol	3.55	1.92	2.98	12.47	43.0	0.42	0.93	0.41	299
n-amyl alcohol	3.43	1.94	2.85	15.80	49.1	0.84	0.86	0.40	299
2-octanol	3.41	1.90	2.84	8.17[a]					310
cyclopentanol	3.44	1.97	2.85	13.90	42.0				300
phenethyl alcohol	3.43	1.94	2.85	13.00	46.7				298
water	3.55	1.88	2.99	78.30	63.1	1.17	0.47	1.09	287

[a] Value for 20 °C (293 K).

TABLE 3: DFT Calculations of Molecular Properties Using B3LYP with the aug-cc-pVDZ Basis Set of Thermodynamic Constants of *R*3MCP in Common Solvents

solvent	μ_{sol}[34] (D)	solvent polarizability[34] (10^{-24} cm^3)	$E_T(30)$[32,33] (kcal/mol)	μ_e (D)	μ_a (D)	$\Delta H°_{calcd}$ (kJ/mol)	$\Delta S°_{calcd}$ [J/(mol K)]
gas phase	–	–	–	3.275	3.297	5.09	0.20
cyclohexane	0.0	10.87	30.9	3.663	3.704	4.34	0.54
toluene	0.375	12.26	33.9	3.738	3.783	4.42	0.57
benzene	0.0	10.32	34.3	3.713	3.756	4.39	0.68
chlorobenzene	1.69	14.1	36.8	4.033	4.101	4.76	1.00
chloroform	1.04	9.5	39.1	3.998	4.063	4.72	1.13
dimethyl sulfoxide	3.96		45.1	4.283	4.375	5.08	1.23
acetonitrile	3.87	4.40	45.6	4.275	4.364	5.04	1.31
ethanol	1.69	5.11	51.9	4.251	4.338	5.00	1.18
methanol	1.70	3.32	55.4	4.270	4.358	5.03	1.26
water	1.854	1.45	63.1	4.305	4.393	4.92	1.21

deduced. The equilibrium constant could thus be determined. As one example, data for acetonitrile are reported in Table 1. A van't Hoff plot, shown in Figure 6 for acetonitrile, was then used to determine the enthalpy and entropy differences between the two conformers. This approach was then successfully applied to 33 other solvents. The resulting enthalpy and entropy differencies are listed in Table 2, along with $\Delta G°$ values at 298 K and λ_{max} values. Selective solvent properties are also presented in Table 2. $E_T(30)$ is an empirically derived parameter that attempts to represent the polarity of a solvent, and α, β, and π^* are interrelated, empirically determined solvent parameters, with α being a measure of a solvent's hydrogen-bond-donating acidity, β being a measure of a solvent's hydrogen-bond-accepting basicity, and π^* being a second measure of solvent polarity. By these criteria, water is a very polar solvent, a very good hydrogen-bond donor, and a moderate hydrogen-bond acceptor. Benzene, on the other hand, is nonpolar, a very poor hydrogen-bond donor, and a weak hydrogen-bond acceptor. It was not possible to carry out the measurements on a neat sample because *R*3MCP is too absorbing through its $n \rightarrow \pi^*$ transition.

Density function calculations were also carried out on the equatorial and axial conformers in solution. The Gaussian package of programs can be used to incorporate the dielectric constant of the solvent directly into calculations of the CD,

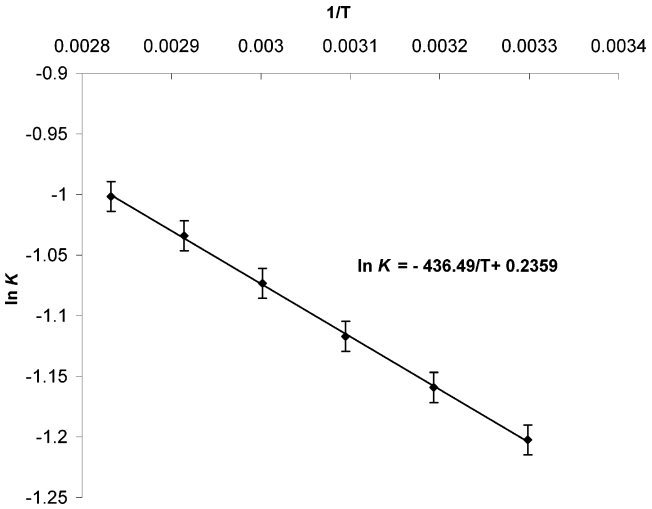

Figure 6. van't Hoff plot for *R*3MCP in acetonitrile solution. The slope represents $\Delta H^\circ = 3.63 \pm 0.05$ kJ/mol, and the *y* intercept yields $\Delta S^\circ = 1.96 \pm 0.10$ J/(mol K).

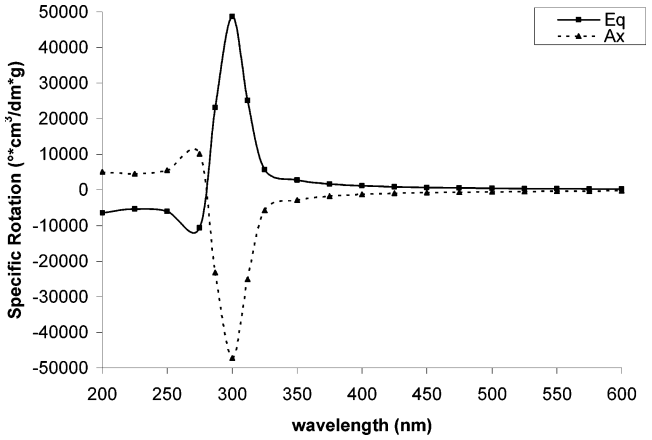

Figure 7. Calculated ORD values for the equatorial and axial conformers of *R*3MCP in cyclohexane obtained using Gaussian 03 density functional calculations with the 6-31G* basis set. The solid and dashed lines are for visual purposes only. The shape of the specific rotation close to and at the exact (singularity) $n \rightarrow \pi^*$ transition is expected to be incorrect. None of the points shown in the figure correspond to exact resonance.

ORD, and thermodynamic constants using a family of models in which the (nonaqueous) solution is referred to as the self-consistent reaction field (SCREF) methods. The solvent is represented as a continuum with a uniform dielectric constant that represents the reaction field. This study specifically employed the polarized continuum model (PCM) originally devised by Tomasi et al.[26−28] This particular model represents the cavity as a series of overlapping and interlocking spheres. The results of these calculations for many of the solvents investigated in this study are listed in Table 3. The solvents were incorporated directly into the calculations of CD, ORD, and thermodynamic constants. The calculated enthalpy differences were typically 1 or 2 kJ/mol higher than the experimental values determined in this study, whereas the calculated entropies had the correct sign of the experimental values but were low by roughly 1 J/(mol K) for each solvent.

The calculated ORD curves are shown in Figure 7 for the equatorial and axial conformers in cyclohexane. These calculations are only valid within the DFT approach using the Gaussian calculations away from resonance (see comment in the figure caption). As was the case for the calculated CD spectra, the two ORD spectra are almost equal in magnitude but opposite

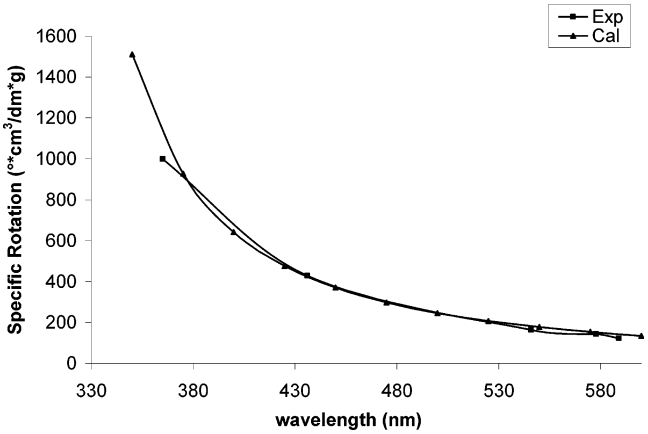

Figure 8. Comparison of the experimental and calculated ORD spectra for *R*3MCP in cyclohexane.

in sign. From these curves and the populations of the conformers determined in cyclohexane, it was possible to calculate the specific rotations of *R*3MCP as a function of wavelength. As seen in Figure 8, the calculated and measured values at five wavelengths are in excellent agreement. This agreement lends credence to the density function calculations and the assumptions that were made to determine populations of conformers.

Finally, in an effort to further assess the computational and experimental methods used for *R*3MCP, we applied these techniques to another often-studied ketone, studying the temperature-dependent CD spectra for *R*-(+)-3-methylcyclohexanone in water solution. A van't Hoff plot yielded a conformer energy difference of $\Delta H^\circ = 3.46 \pm 0.05$ kJ/mol. This value lies in the middle of a range of values reported earlier using different methods by Djerassi et al.[29] (3.3 kJ/mol), Robins and Walker[30] (3.8 kJ/mol), and Lightner and Crist (4.0−5.0 kJ/mol).[31] Given the differences in the values for various methods, one might conclude that it is possible to determine ΔH° within ~1 kJ/mol from van't Hoff analysis.

Conclusions

Temperature-dependent electronic circular dichroism (CD) spectra are reported herein for (*R*)-(+)-3-methylcyclopentanone (*R*3MCP) in 34 solvents. The differences in enthalpy values determined in this study are ~1 kJ/mol lower than those measured in the gas phase[19] and for the pure compound but within the expected uncertainties of such measurements.[3] A comparison of similar data using a variety of methods for *R*-(+)-3-methylcyclohexanone was also found to be within this range of uncertainty. Vibrational fine structure in the CD of the $n \rightarrow \pi^*$ transition was observed in the gas phase as well as in solvents of low polarity. The λ_{max} value for the CD of the $n \rightarrow \pi^*$ transition decreases approximately linearly as the polarity of the solvent increases, as observed for many other systems. What is most striking about the ΔH° and ΔS° data in Table 2 is that there is no obvious strong correlation between the thermodynamic quantities and solvent properties such as dielectric constant, polarizability, and polarity.[32] On the contrary, the calculated enthalpies presented in Table 3 increase slightly (by approximately 0.7 kJ/mol from 0 to 4 D) with increasing dipole moment of the solvent. The experimental data do show higher values of ΔH° for the polar solvents with the highest moments, but the scatter in the data does not predict a general trend as seen in the calculations. Calculated entropy differences also correlate with solvent polarity: In nonpolar media such as the gas phase, cyclohexane, benzene, and toluene, the entropy

differences are small, whereas in polar media such as water, dimethyl sulfoxide, and acetonitrile, the values are larger. The calculations likewise give similar values and are ~1 kJ/mol greater than experiment. Perhaps the lack of a correlation between the measured thermodynamic quantities and solvent polarities is a reflection of the fact that the dipole moments of the equatorial and axial conformers are virtually identical, independent of solvent (Table 3). We conclude that the precision of the experimental data at this point is insufficient to detect the small changes predicted by theory.

Acknowledgment. This research was supported by the National Science Foundation (CHE-0094815). We also acknowledge Dr. R. J. Hinde for theoretical assistance.

References and Notes

(1) Dzakua, Z.; DeRider, M. L.; Markley, J. L. *J. Am. Chem. Soc.* **1996**, *118*, 12796.
(2) Brutcher, F. V., Jr.; Roberts, T.; Barr, S. J.; Pearson, N. *J. Am. Chem. Soc.* **1959**, *81*, 4915.
(3) He, J.; Petrovic, A. G.; Polavarapu, P. L. *J. Phys. Chem. B* **2004**, *108*, 20451.
(4) Boese, R.; Oberhammer, H.; Pulay, P.; Waterfeld, A. *J. Phys. Chem.* **1993**, *38*, 9625.
(5) Mislow, K.; Bunnenber, E.; Records, R.; Wellman, K.; Djerassi, C. *J. Am. Chem. Soc.* **1962**, *84*, 1342.
(6) Wellman, K.; Bunnenber, E.; Djerassi, C. *J. Am. Chem. Soc.* **1963**, *85*, 1870.
(7) Moscowitz, A.; Wellman, K. Djerassi, C. *J. Am. Chem. Soc.* **1963**, *85*, 3515.
(8) Moscowitz, A.; Wellman, K. Djerassi, C. *Proc. Natl. Acad. Sci.* **1963**, *50*, 799.
(9) Wellman, K.; Records, R.; Bunnenberg, E.; Djerassi, C. *J. Am. Chem. Soc.* **1963**, *85*, 492.
(10) Wellman, K.; Djerassi, C. *J. Am. Chem. Soc.* **1964**, *86*, 1964.
(11) Wellman, K.; Laur, P. H. A.; Briggs, W. S.; Moscowitz, A.; Djerassi, C. *J. Am. Chem. Soc.* **1965**, *87*, 66.
(12) Wellman, K.; Briggs, W. S.; Djerassi, C. *J. Am. Chem. Soc.* **1964**, *86*, 73.
(13) Kirk, D. N.; Kyle, W.; Wallis, S. R. *J. Chem. Soc. C* **1970**, 350.
(14) Lightner, D. A.; Bouman, T. D.; Wijekoon, W. M. D.; Hansen, A. E. *J. Am. Chem. Soc.* **1986**, *108*, 4484.
(15) Li Y. S. *J. Mol. Spectrosc.* **1984**, *104*, 302.
(16) Richardson, F. S.; Shillady, D. D.; Bloor, J. E. *J. Phys. Chem.* **1971**, *75*, 2466.
(17) Flament, J. P.; Gervais, J. P. *Tetrahedron* **1980**, *36*, 1949.
(18) Potts, A. R.; Nesselrodt, D. R.; Baer, T.; Driscoll, J. W.; Philip, J. *J. Phys. Chem.* **1995**, *99*, 12090.
(19) Kim, D.; Baer, T. *Chem. Phys.* **2000**, *256*, 251.
(20) Li, R.; Sullivan, R.; Al-Basheer, W.; Pagni, R. M.; Compton, R. N. *J. Chem. Phys.* **2006**, *125*, 144304.
(21) Fischer, A. T.; Compton, R. N.; Pagni, R. M. *J. Phys. Chem. A* **2006**, *110*, 7067.
(22) Frisch, M. J.; Trucks, G. W.; Schlegel, H. B.; Scuseria, G. E.; Robb, M. A.; Cheeseman, J. R.; Montgomery, J. A., Jr.; Vreven, T.; Kudin, K. N.; Burant, J. C.; Millam, J. M.; Iyengar, S. S.; Tomasi, J.; Barone, V.; Mennucci, B.; Cossi, M.; Scalmani, G.; Rega, N.; Petersson, G. A.; Nakatsuji, H.; Hada, M.; Ehara, M.; Toyota, K.; Fukuda, R.; Hasegawa, J.; Ishida, M.; Nakajima, T.; Honda, Y.; Kitao, O.; Nakai, H.; Klene, M.; Li, X.; Knox, J. E.; Hratchian, H. P.; Cross, J. B.; Bakken, V.; Adamo, C.; Jaramillo, J.; Gomperts, R.; Stratmann, R. E.; Yazyev, O.; Austin, A. J.; Cammi, R.; Pomelli, C.; Ochterski, J. W.; Ayala, P. Y.; Morokuma, K.; Voth, G. A.; Salvador, P.; Dannenberg, J. J.; Zakrzewski, V. G.; Dapprich, S.; Daniels, A. D.; Strain, M. C.; Farkas, O.; Malick, D. K.; Rabuck, A. D.; Raghavachari, K.; Foresman, J. B.; Ortiz, J. V.; Cui, Q.; Baboul, A. G.; Clifford, S.; Cioslowski, J.; Stefanov, B. B.; Liu, G.; Liashenko, A.; Piskorz, P.; Komaromi, I.; Martin, R. L.; Fox, D. J.; Keith, T.; Al-Laham, M. A.; Peng, C. Y.; Nanayakkara, A.; Challacombe, M.; Gill, P. M. W.; Johnson, B.; Chen, W.; Wong, M. W.; Gonzalez, C.; Pople, J. A. *Gaussian 03*, revision B.03; Gaussian, Inc.: Pittsburgh, PA, 2003.
(23) Ballard, R. E.; Mason, S. F.; Vane, G. W. *Discuss. Faraday Soc.* **1963**, *35*, 43.
(24) Temperature-dependent CD spectra of *R*3MCP are shown in ref 20.
(25) Jaffé, H.; Orchin, M. *Theory and Applications of Ultraviolet Spectroscopy*; Wiley: New York, 1962.
(26) Miertus, S.; Scrocco, E.; Tomasi, J. *Chem. Phys.* **1981**, *55*, 117.
(27) Miertus, S.; Tomasi, J. *Chem. Phys.* **1992**, *65*, 239.
(28) Cossi, M.; Barone, V.; Cammi, R.; Tomasi, J. *Chem. Phys. Lett.* **1996**, *255*, 327.
(29) Djerassi, C.; Warawa, E. J.; Berdahl, J. M.; Eisenbraun, E. J. *J. Am. Chem. Soc.* **1961**, *83*, 3334.
(30) Robins, P. A.; Walker, *J. Chem. Ind. (London)* **1955**, 772.
(31) Lightner, D. A.; Crist, B. V. *Appl. Spectrosc.* **1979**, *33*, 3.
(32) Reichardt, C. *Solvents and Solvent Effects in Organic Chemistry*, 3rd ed.; Wiley-VCH: Weinheim, Germany, 2003.
(33) Marcus, Y. *The Properties of Solvents*; 1998.
(34) *Handbook of Chemistry and Physics*, 68th ed.; Lide, D. R., Ed.; CRC Press: Boca Raton, FL, 1987−1988.